Recent progress of graphene orientation determination technology based on scanning probe microscopy

Yu Zhang ✉, *Guangjie Liu* ✉, *Wenjing Xu*

Department of Computer Science and Technology, Changchun Normal University, Changchun 130032, People's Republic of China
✉ *E-mail: zhangyu@mail.cncnc.edu.cn, 756058599@qq.com*

Published in Micro & Nano Letters; Received on 6th January 2020; Revised on 18th March 2020; Accepted on 23rd March 2020

Graphene is regarded as an excellent substitute for silicon and an ideal chip material for the next generation of chip manufacturing. Researches show that the electrical properties of graphene are closely related to its edge structures. Graphene can exhibit metal or semiconductive characteristics according to the different edge configurations. How to fabricate graphene nanoribbons with specific edge structures is the key premise for practical applications. The review highlights the new graphene crystal orientation detection methods based on scanning probe technology, including offline detection technology and online detection technology. The advantages and disadvantages of different detection technologies are analysed, and finally, a brief outlook for the development of graphene orientation determination techniques is given.

1. Introduction: With the development of the miniaturisation process, it's more and more difficult to manufacture chips with smaller sizes and lower costs [1–4]. Moore's law is coming to an end [5]. The research on new materials and new technologies has become a hot topic in the world. Graphene has attracted considerable attention in different fields in recent years [6–9]. It enables the frequency of the processor more than 1 THz, which is 100–000 times higher than the current silicon-based processor [10, 11]. The RF transistors made by graphene are huge faster than the most advanced silicon transistors with the same gate length [12, 13]. However, the graphene-based transistors cannot be completely switched off. Therefore, it's necessary to introduce a bandgap into the intrinsic graphene for fabricating graphene-based semiconductor devices. Theoretical and experimental studies show that manufacturing graphene into nanoribbons or quantum dots could introduce bandgaps [14–16]. Graphene shows metallic or semiconductive characteristics according to the different geometry configurations and edge structures [17–19]. Therefore, how to patterning graphene nanoribbons with specific edge structures is the key premise and current hot research topic. Consequently, the graphene orientation detection is the key to the fabrication of graphene-based nanodevices. To date, researchers have done a lot of research on it and made some important progress.

This review overviews the recent advances in the graphene crystal orientation detection methods based on scanning probe technology, including offline detection technology and online detection technology. Furthermore, the advantages and disadvantages of different detection technologies are discussed. In the last part, the future development of graphene orientation detection techniques has prospected

2. Offline determination technique

2.1. Scanning tunneling microscope (STM)

2.1.1. STM imaging of graphite: STM images the charge density of electrons at the Fermi level. When all surface atoms of materials form a local maximum of charge density at Fermi level, all surface atoms can be observed by STM. However, if there are different types of surface atoms in materials, STM can only observe one type of surface atoms, such as GaAs(110). As atoms can only be observed at the negative bias, while Ga atoms can only be observed at the positive bias. Graphite has two types of C atoms in the lattice, as shown in Fig. 1*a*, which are α and β atoms, respectively. According to the polarity of bias voltage, only one type of C atom can be observed. In the early studies of graphite atomic resolution imaging, a triangular structure was displayed in the atomic resolution image, as shown in Fig. 1*b*. Only one type atom is observed, and the other type atom is in the 'hidden' state, with an atomic period of 0.25 nm.

Early theoretical researches demonstrated that only β atom could be observed by STM [20, 21]. Wang *et al.* [21] found that the local density of states (LDOS) at the Fermi level of β atom is higher than that of α atom, so β atom is more easily observed by STM. Subsequently, both of the triangular structure and the hexagonal lattice structure can be observed [22]. Mizes *et al.* [23] thought that it was caused by a multiprobe effect. While Wang *et al.* [21] and Paredes *et al.* [24] considered that it was caused by the lateral sliding between layers without rotation. Moriarty and Hughes [25] believed that the hexagonal lattice structure would only appear under certain conditions, such as applying pulse signals on the probe.

2.1.2. STM imaging of graphene made by mechanical exfoliation: The atomic structures of monolayer graphene prepared by mechanical exfoliation were observed by STM in 2007 [26]. Graphene prepared by mechanical exfoliation is usually transferred onto a SiO_2 substrate. STM imaging requires that the substrate must be conductive, so it's necessary to deposit electrodes on graphene and SiO_2 substrate. Therefore, the imaging result is worse than that of the conductive substrate. The original image measured in the experiment is relatively fuzzy, as shown in Fig. 2*a*. After high-pass filtering of the original image, the triangular structure, and hexagonal structure can be displayed, as shown in Fig. 2*b*. The quality of atomic resolution imaging can be improved by pretreatment of graphene samples [27].

The monolayer graphene and the multilayer graphene on the insulating substrate were observed in the ultra-high vacuum condition at liquid nitrogen temperature. The monolayer graphene shows a hexagonal lattice structure, as shown in Fig. 2*c*, and multilayer graphene shows a triangular structure, as shown in Fig. 2*d*. Also, the hexagonal lattice structure can be observed by changing the STM imaging conditions. Murata *et al.* [28] imaged the graphene on the SiC substrate by constantly changing the bias voltage. When the bias voltage was + 0.1 V, the hexagonal lattice structure can be observed.

Different researchers give different conclusions and reasons for graphene STM imaging results. Stolyarova *et al.* [27] considered

that the atoms of the bilayer and multilayer graphenes are the same as that of graphite, i.e. the surface C atoms are different. Therefore, STM observation results are the same as that of graphite. There can be two kinds of atomic images, triangular structures, and hexagon structures. However, all surface C atoms are the same in monolayer. The lattice defects, the interaction with the substrate, and the winkles of monolayer graphene will cause obvious fluctuation of local electron density, which will affect STM imaging. Because the strong space disturbance affects the electronic state of graphene, triangular structures and hexagonal structures can be both observed on the monolayer graphene [26].

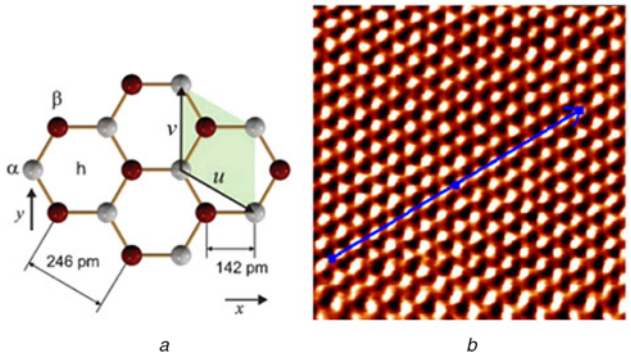

Fig. 1 *STM imaging of graphite*
a Lattice structure of graphite [20]
b STM image of HOPG [21]

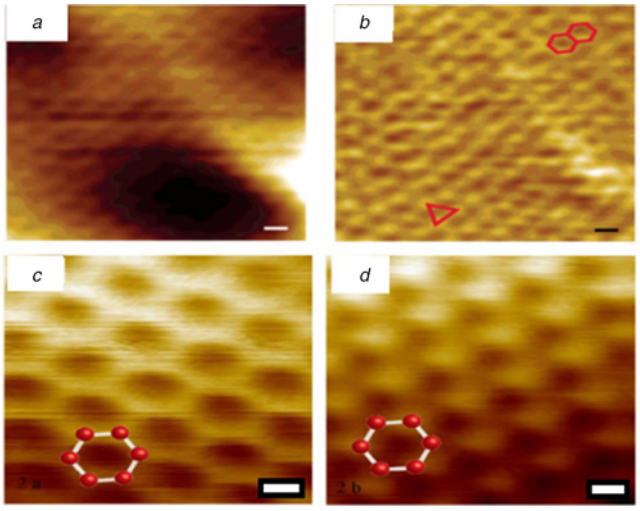

Fig. 2 *STM images of graphene*
a Original STM image of graphene with a fuzzy atomic structure. The scale bar is 0.25 nm [26]
b High-pass filtered image of (a), with triangular structures and hexagonal structures. The scale bar is 0.25 nm [26]
c STM atomic image of monolayer graphene. The scale bar is 0.1 nm [27]
d STM atomic image of multilayer graphene. The scale bar is 0.1 nm [27]

2.1.3. STM imaging principle of CVD graphene: CVD method can directly grow large areas of graphene on metal or semiconductive substrates, and many researchers use STM to study its growth mechanism. Experimental research shows that graphene and the substrates can be imaged separately according to different tunnelling conditions [29]. The hexagonal lattice structures of graphene were shown at low voltage, and the lattice structures of the germanium substrate were displayed at high voltage. STM can not only image the flat areas, but also rough regions with atomic resolution, such as defects, edges, wrinkles, and boundaries of graphene. The atomic structures of edges and winkles of graphene were studied [30, 31]. The experiments performed in a UHV at room temperature. Atomic resolution images of a single vacancy and the flower defects in graphene lattice were reported [32, 33]. Moreover, atomic structures of the grain boundaries with different configurations in graphene were demonstrated [34, 35].

2.2. Atomic force microscope (AFM): Theoretically, all surface atoms of materials can be observed by AFM. Because AFM measures not the charge density of electrons at the Fermi level, but the total charge density of electrons. The phenomenon of stick-slip on the surface of graphite was observed for the first time in an ultra-high vacuum condition, and the atomic resolution image of graphite was obtained [36]. AFM can not only obtain atomic-resolution images, but also operate the samples, such as cutting. It can also be used to study the friction at the atomic scale. Therefore, AFM is the only tool that can image and manipulate any material at meanwhile. AFM has two different imaging modes for atomic resolution imaging: non-contact mode (nc-AFM) and contact mode.

2.2.1. nc-AFM mode: In the nc-AFM mode, the tip of the AFM does not contact with the sample during the imaging process, and the imaging is performed by detecting the changes of the resonance frequency of the probe. Accordingly, the lateral resolution is lower than the contact mode. Moreover, the imaging conditions are relatively strict, and it's generally difficult to achieve atomic resolution images in the atmospheric environment at room temperature [37]. Because the imaging resolution is closely related to the atomic shape of the AFM probe and the distance between the probe and the sample, there are two methods to improve the imaging resolution. The sub-angstrom amplitude of the probe

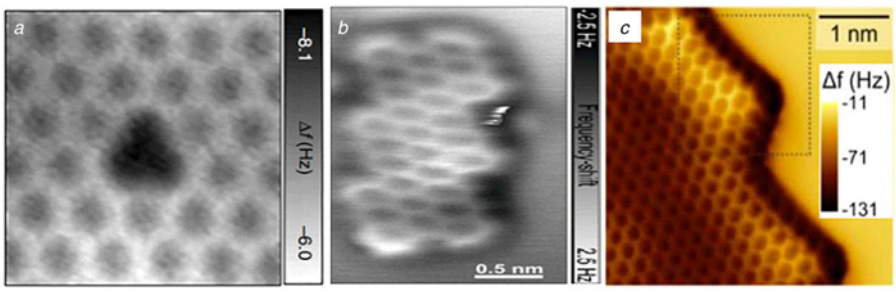

Fig. 3 *nc-AFM atomic imaging of rough region on graphene*
a Constant-height AFM atomic image of a single N-dopant in graphene [41]
b nc-AFM frequency-shift image of a short and flat GNR at the constant height [39]
c Atomic image of a graphene edge measured with an iridium-terminated tip [38]

doi: 10.1049/mnl.2019.0782

could enhance the sensitivity of the short-range force to enhance the spatial resolution [38]. In addition, the spatial resolution further improved by adsorbing atoms or functionalising inorganic small molecules on the AFM probe [38–42]. Boneschanscher *et al.* [38] studied these two methods. The results demonstrated different structures have shown at different tip-sample distances d_{ts}.

In compared with the contact mode, nc-AFM can image both of the flat regions and the regions with small fluctuations, such as doping structures and edge structures. Fig. 3*a* shows the atomic resolution image of a single nitrogen-doped graphene by using a CO-terminated probe. Fig. 3*b* is the atomic resolution images of graphene nanoribbons with a CO-terminated tip. It presented that the edge structure of the nanoribbons is zigzag. Fig. 3*c* shows that the edge structure of graphene island is zigzag using an iridium-terminated tip.

2.2.2. Contact mode: In the contact mode, the AFM tip always keeps contacting with the samples, and the scanning angle is usually 90° or 270°. This imaging mode is called lateral force microscopy (LFM) [43]. Using this method, both of the atomic resolution images of the sample and the friction information are saved during the imaging process. It's relatively easy to obtain atomic-resolution images using LFM mode. In the early stage, the imaging conditions of the contact mode were stringent [43–45]. Until 2010, Lee *et al.* [46] obtained the atomic resolution images of graphite and graphene in the atmospheric environment. Both graphene and graphite show triangular structures.

In 2014, Zhang *et al.* [47] reported atomic resolution images of graphene in an atmospheric environment at room temperature. Meanwhile, friction forces with different scan angles were obtained. To remove the tip effect of the probe, the sample rotation was used to keep the scanning angle of the probe unchanged [48]. Both of these two works show that the friction force changes in 60° period as the lattice period of graphene, and the friction force along armchair orientation is greater than that along with the zigzag orientation, as shown in Fig. 4.

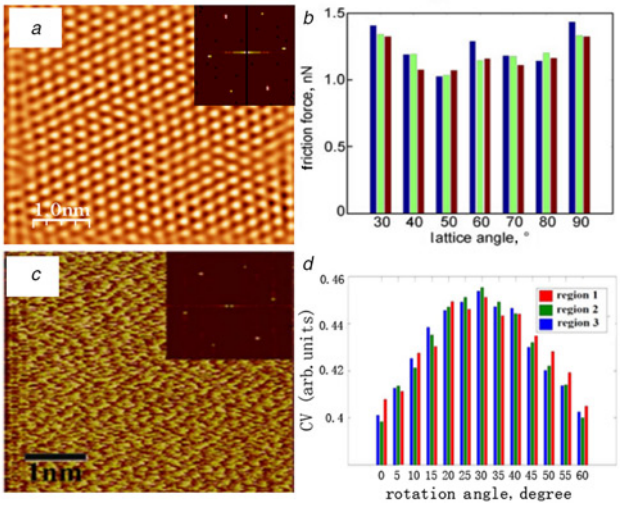

Fig. 4 *Friction of graphene*
a Filtered image of multilayer graphene by FFT [47]
b Friction force is measured three times at each angle with different colour bars [47]
c Filtered images of monolayer graphene [48]
d Coefficient of variation versus rotation angle for three regions showing 60° periodicity [48]

3. Online determination technique: The technology of graphene orientation detection mentioned above can only be used for offline structure observation. It's difficult to relocate and align the machining position for cutting graphene with special edge structures. In order to solve these issues, Zhang *et al.* [49] proposed a fast graphene orientation detection method through lateral forces. Using only one or two friction scanning lines, the lattice orientation of graphene can be detected quickly and accurately before graphene manufacturing. This method is online monitoring, which effectively overcomes the problem of machining position alignment. The intrinsic spatial frequency and the lattice angle distribution of graphene are shown in Fig. 5*a*. The results show that there is only one frequency peak when the probe moves along zigzag orientation. When the probe moves along armchair orientation, there are two different frequency peaks. There are three different frequency peaks when $0°<\theta<30°$ or $30°<\theta<60°$. Therefore, zigzag or armchair orientations can be determined by only one friction scanning line. According to the formula of the frequency ratio δ and angle θ, the orientations between zigzag and armchair can be judged. Fig. 5*b* displays the distribution between the experimental, theoretical frequency ratio and lattice angles. $L=58$, $L=116$ and $L=216$ are experimental results. The red bars show the theoretical results. The frequency spectrum distribution varies with different lattice orientations: single, double and three peaks. This technology can be easily applied to other two-dimensional materials. Li *et al.* [50] applied it to determine the lattice orientation of MoS_2 using single-line scan power spectrum analysis. The experiment results show that this method is effective and convenient.

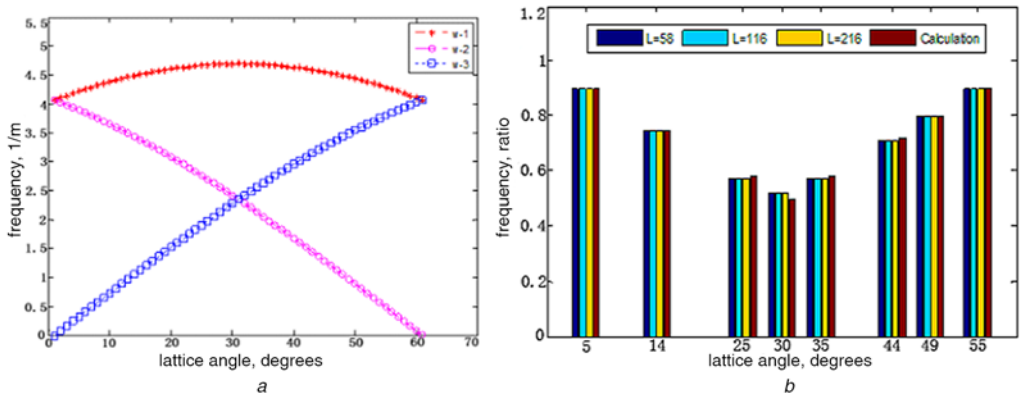

Fig. 5 *Relationship of the lattice angles and spatial frequencies [49]*
a Distribution between the spatial frequencies and lattice angles
b Distribution between the experimental, theoretical frequency ratio and lattice angles

4. Conclusion: This review summary the recent researches on graphene orientation determination methods based on scanning probe microscopy. These methods could be divided into two categories: offline technique and online determination technique. Offline methods have the challenges of machining position relocation and alignment. AFM enables realising the online graphene orientation detection. However, it only enables detecting the orientation of single-crystalline graphene so far. In the future, this online determination technique is expected to detect the orientation of polycrystalline graphene and the graphene with structural defects, which meets the practical applications of graphene device manufacturing.

5. Acknowledgments: This work supported by the National Natural Science Foundation of China (grant no. 61604019), the talent introduction scientific research project of Changchun Normal University, China (grant no. RC2016009).

6 References

[1] Huang Q.H.: 'International technology roadmap for semiconductors (2013 edition)', *China Integr. Circuit*, 2014, **23**, (9), pp. 25–45
[2] Young K.K.: 'Short-channel effect in fully depleted SOI MOSFET's', *IEEE Trans. Electron Devices*, 1989, **36**, (2), pp. 399–402
[3] Chaudhry A., Kumar M.J.: 'Controlling short-channel effects in deep-submicron SOI MOSFETs for improved reliability: a review', *IEEE Trans. Device Mater. Reliab.*, 2004, **4**, (1), pp. 99–109
[4] Gao X., Liou J.J., Wong W., *ET AL.*: 'An improved electrostatic discharge protection structure for reducing triggering voltage and parasitic capacitance', *Solid. State. Electron.*, 2003, **47**, (6), pp. 1105–1110
[5] Waldrop M. M.: 'The chips are down for Moore's law', *Nature*, 2016, **530**, pp. 145–147
[6] Ahmadian M., Sharifi M.J.: 'A diagrammatic approach to single-electron spintronics and a new analytical model for ferromagnetic single-electron transistors', *AEU-Int J. Electron. C*, 2019, **102**, pp. 62–68
[7] Ahmadian M., Jafari K., Sharifi M.J.: 'Novel graphene-based optical MEMS accelerometer dependent on intensity modulation', *ETRI J.*, 2018, **40**, (4), pp. 1–8
[8] Fu W., Makk P., Maurand R., *ET AL.*: 'Large-scale fabrication of BN tunnel barriers for graphene spintronics', *J. Appl. Phys.*, 2014, **116**, p. 074306
[9] Ahmadian M., Jafari K.: 'A graphene-based wide-band MEMS accelerometer sensor dependent on wavelength modulation', *IEEE Sens. J.*, 2019, **19**, pp. 6226–6232
[10] Katsnelson M. I.: 'Graphene: carbon in two dimensions', *Mater. Today*, 2007, **10**, (1–2), pp. 20–27
[11] Balandin A.A., Ghosh S., Bao W., *ET AL.*: 'Superior thermal conductivity of single-layer graphene', *Nano Lett.*, 2008, **8**, (3), pp. 902–907
[12] Wu Y., Lin Y.M., Bol A.A., *ET AL.*: 'High-frequency, scaled graphene transistors on diamond-like carbon', *Nature*, 2011, **472**, pp. 74–78
[13] Han S.J., Garcia A.V., Oida S., *ET AL.*: 'Graphene radio frequency receiver integrated circuit', *Nat. Commun.*, 2014, **5**, p. 3086
[14] Yao X., Niu X., Ma K., *ET AL.*: 'Graphene quantum dots-capped magnetic mesoporous silica nanoparticles as a multifunctional platform for controlled drug delivery, magnetic hyperthermia, and photothermal therapy', *Small*, 2017, **13**, (2), p. 1602225
[15] Talirz L., Söde H., Dumslaff T., *ET AL.*: 'On-surface synthesis and characterization of 9-atom wide armchair graphene nanoribbons', *ACS Nano*, 2017, **11**, (2), pp. 1380–1388
[16] Heerema S.J., Dekker C.: 'Graphene nanodevices for DNA sequencing', *Nat. Nanotechnol.*, 2016, **11**, (2), pp. 127–136
[17] Zhu W., Neumayer D., Perebeinos V., *ET AL.*: 'Silicon nitride gate dielectrics and band gap engineering in graphene layers', *Nano Lett.*, 2010, **10**, (9), pp. 3572–3576
[18] Ouyang F., Peng S., Liu Z., *ET AL.*: 'Bandgap opening in graphene antidot lattices: the missing half', *ACS Nano*, 2011, **5**, (5), pp. 4023–4030
[19] Feng J., Li W., Qian X., *ET AL.*: 'Patterning of graphene', *Nanoscale*, 2012, **4**, (16), pp. 4883–4899
[20] Hembacher S., Giessibl F.J., Mannhart J., *ET AL.*: 'Revealing the hidden atom in graphite by low-temperature atomic force microscopy', *Proc. Natl. Acad. Sci.*, 2003, **100**, (22), pp. 12539–12542
[21] Wang Y., Ye Y., Wu K.: 'Simultaneous observation of the triangular and honeycomb structures on highly oriented pyrolytic graphite at room temperature: an STM study', *Surf. Sci.*, 2006, **600**, (3), pp. 729–734
[22] Wong H.S., Durkan C., Chandrasekhar N.: 'Tailoring the local interaction between graphene layers in graphite at the atomic scale and above using scanning tunneling microscopy', *ACS Nano*, 2009, **3**, (11), pp. 3455–3462
[23] Mizes H.A., Park S., Harrison W.A.: 'Multiple-tip interpretation of anomalous scanning tunneling microscopy images of layered materials', *Phys. Rev. B*, 1987, **36**, (8), pp. 4491–4494
[24] Paredes J.I., Martinez-Alonso A., Tascon J.M.D.: 'Triangular versus honeycomb structure in atomic-resolution STM images of graphite', *Carbon. N. Y.*, 2001, **39**, (3), pp. 476–479
[25] Moriarty P., Hughes G.: 'Atomic resolved material displacement on graphite surfaces by scanning tunnelling microscopy', *Appl. Phys. Lett.*, 1992, **60**, (19), pp. 2338–2340
[26] Ishigami M., Chen J.H., Cullen W.G., *ET AL.*: 'Atomic structure of graphene on SiO_2', *Nano Lett.*, 2007, **7**, (6), pp. 1643–1648
[27] Stolyarova E., Rim K.T., Ryu S., *ET AL.*: 'High-resolution scanning tunneling microscopy imaging of mesoscopic graphene sheets on an insulating surface', *Proc. Natl. Acad. Sci.*, 2007, **104**, (22), pp. 9209–9212
[28] Murata Y., Cavallucci T., Tozzini V., *ET AL.*: 'Atomic and electronic structure of Si dangling bonds in quasi-free-standing monolayer graphene', *Nano Res.*, 2018, **11**, (2), pp. 864–873
[29] Dai J., Wang D., Zhang M., *ET AL.*: 'How graphene islands are unidirectionally aligned on the Ge(110) surface', *Nano Lett.*, 2016, **16**, (5), pp. 3160–3165
[30] Gao T., Xie S., Gao Y., *ET AL.*: 'Growth and atomic-scale characterizations of graphene on multifaceted textured Pt foils prepared by chemical vapor deposition', *ACS Nano*, 2011, **5**, (11), pp. 9194–9201
[31] Tian J., Cao H., Wu W., *ET AL.*: 'Direct imaging of graphene edges: atomic structure and electronic scattering', *Nano Lett.*, 2011, **11**, (9), pp. 3663–3668
[32] Ugeda M.M., Fernandez-Torre D., Brihuega I., *ET AL.*: 'Point defects on graphene on metals', *Phys. Rev. Lett.*, 2011, **107**, (11), p. 116803
[33] Yan H., Liu C.C., Bai K.K., *ET AL.*: 'Electronic structures of graphene layers on a metal foil: the effect of atomic-scale defects', *Appl. Phys. Lett.*, 2013, **103**, (14), p. 143120
[34] Yang B., Xu H., Lu J., *ET AL.*: 'Periodic grain boundaries formed by thermal reconstruction of polycrystalline graphene film', *J. Am. Chem. Soc.*, 2014, **136**, (34), p. 12041
[35] Ma C., Sun H., Zhao Y., *ET AL.*: 'Evidence of van hove singularities in ordered grain boundaries of graphene', *Phys. Rev. Lett.*, 2014, **112**, (24), p. 226802
[36] Mate C.M., McClelland G.M., Erlandsson R., *ET AL.*: 'Atomic-scale friction of a tungsten tip on a graphite surface', *Phys. Rev. Lett.*, 1987, **59**, (17), pp. 1942–1945
[37] Liu Y., Weinert M., Li L.: 'Determining charge state of graphene vacancy by noncontact atomic force microscopy and first-principles calculations', *Nanotechnology*, 2015, **26**, (3), p. 035702
[38] Boneschanscher M.P., Van der Lit J., Sun Z., *ET AL.*: 'Quantitative atomic resolution force imaging on epitaxial graphene with reactive and nonreactive AFM probes', *ACS Nano*, 2012, **6**, (11), pp. 10216–10221
[39] Sánchez-Sánchez C., Dienel T., Deniz O., *ET AL.*: 'Purely armchair or partially chiral: noncontact atomic force microscopy characterization of dibromo-bianthryl-based graphene nanoribbons grown on Cu (111)', *ACS Nano*, 2016, **10**, (8), pp. 8006–8011
[40] Gross L., Mohn F., Moll N., *ET AL.*: 'The chemical structure of a molecule resolved by atomic force microscopy', *Science*, 2009, **325**, pp. 1110–1114
[41] Torre B., Švec M., Hapala P., *ET AL.*: 'Non-covalent control of spin-state in metal-organic complex by positioning on N-doped graphene', *Nat. Commun.*, 2018, **9**, (1), pp. 1–9
[42] Ruffieux P., Wang S., Yang B., *ET AL.*: 'On-surface synthesis of graphene nanoribbons with zigzag edge topology', *Nature*, 2016, **531**, pp. 489–492
[43] Sumomogi T., Hieda K., Endo T., *ET AL.*: 'Influence of atmosphere humidity on tribological properties in scanning probemicroscope observation', *Appl. Phys. A Mater. Sci. Process.*, 1998, **66**, pp. 299–303
[44] Sokolov I.Y., Henderson G.S., Wicks F.J.: 'Theoretical and experimental evidence for 'true' atomic resolution under non-vacuum conditions', *J. Appl. Phys.*, 1999, **86**, (10), pp. 5537–5540
[45] Kostić R., Mirić M., Radić T., *ET AL.*: 'Optical characterization of graphene and highly oriented pyrolytic graphite', *Acta Phys. Pol. A*, 2009, **116**, (4), pp. 718–721
[46] Lee C., Li Q., Kalb W., *ET AL.*: 'Frictional characteristics of atomically thin sheets', *Science*, 2010, **328**, pp. 76–80

doi: 10.1049/mnl.2019.0782

[47] Zhang Y., Liu L., Xi N., *ET AL.*: 'Friction anisotropy dependence on lattice orientation of graphene', *Sci. Chin. Phys., Mech. Astron.*, 2014, **57**, (4), pp. 663–667
[48] Liu Z., Ma T., Liu L.: 'Optical-assistant characterization of friction anisotropy properties of single-crystal graphene domains', *Tribol. Int.*, 2017, **110**, pp. 131–139
[49] Zhang Y., Yu F., Li G., *ET AL.*: 'Online determination of graphene lattice orientation through lateral forces', *Nanoscale Res. Lett.*, 2016, **11**, (1), p. 353
[50] Li M., Zhang Y., Yu P., *ET AL.*: ' a novel and facile method for detecting the lattice orientation of MoS_2 tribological surface using the SPSA process', *Mater. Des.*, 2017, **135**, pp. 291–299